https://doi.org/10.5194/egusphere-2026-800
Preprint. Discussion started: 18 March 2026

Investigation of supercooled water droplet sticking efficiency during power transmission line icing using digital holography

Pu Zhang, Dengxin Hua, Jiang Cheng, Jingjing Liu, Xiang Xu, Yitong Miao, Jun Wang*

Xi'an University of Technology, Xi'an, China

Correspondence to: Jun Wang (wangjun790102@xaut.edu.cn)

Abstract. Transmission line icing severely threatens the safety of the power grid. Accurate prediction of the sticking efficiency (the proportion of supercooled droplets that remain on the conductor after impact, excluding bouncing and splashing) is critical for preventing and mitigating icing disasters. Traditional prediction models for sticking efficiency typically exhibit significant errors under complex conditions (e.g. varying wind speeds and precipitation intensities), thereby limiting their practical applications. To overcome this drawback, a multi-stage coupled model based on coaxial digital holography was proposed, in which supercooled droplet diameters, velocities, and collision angles were precisely measured. These measurements were integrated into a multi-stage framework that couples droplet impact dynamics and thermodynamics to compute the sticking efficiency, thereby overcoming the accuracy limitations of existing models in complex environments. Experimental results show that the new model's prediction errors remain below 3.5% across a range of conditions, which is a significant improvement over traditional models, underscoring its enormous potential in engineering applications.

Keywords: transmission line icing; sticking efficiency; digital holography; multi-stage coupling model

https://doi.org/10.5194/egusphere-2026-800
Preprint. Discussion started: 18 March 2026

Graphical abstract

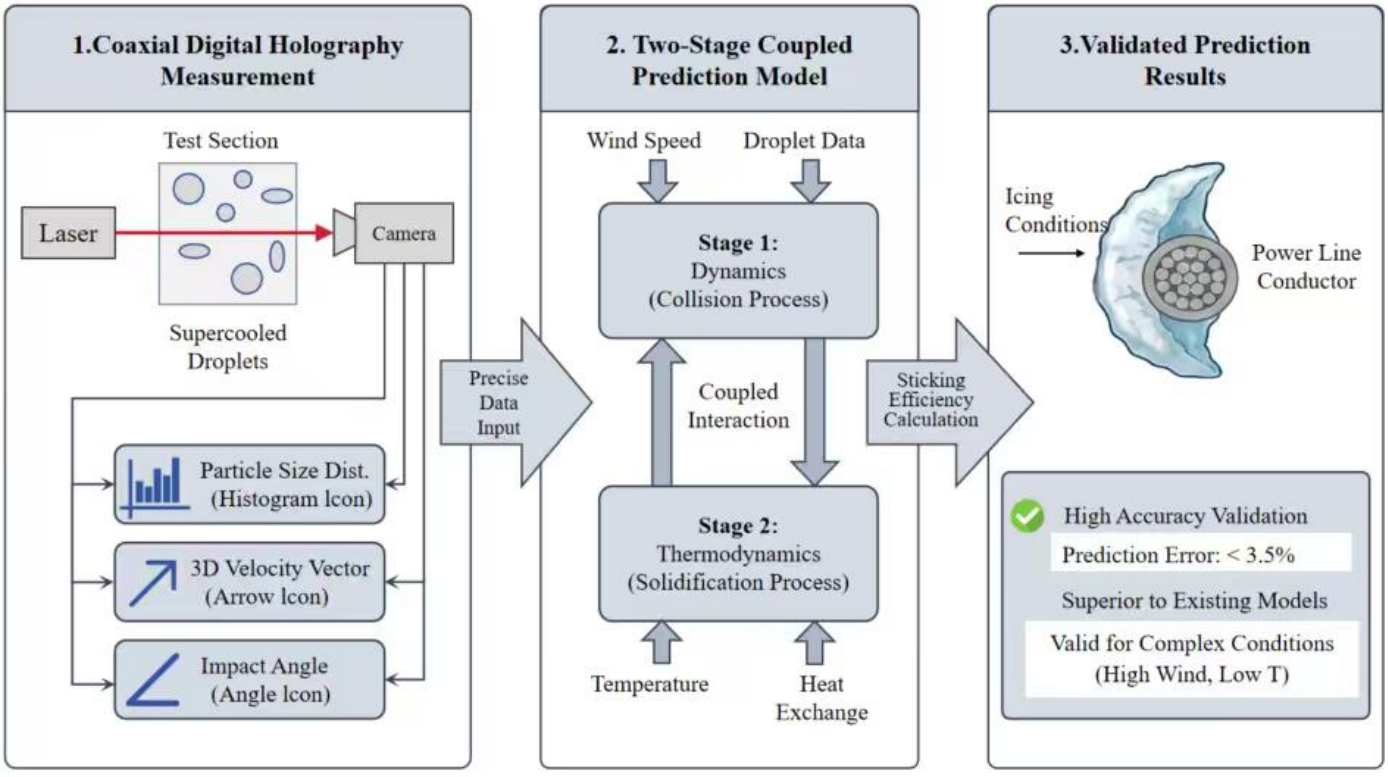

1 Introduction

Accidents (such as tower collapses, wire breakages, and flashover trips) caused by transmission line icing seriously threaten the safety of power grids. Therefore, accurately predicting transmission line icing conditions is crucial for preventing and mitigating ice-related disasters (Wang et al., 2024). Among various prediction methods, physical icing models are considered the most precise paradigm for predicting transmission line icing, and the accurate calculation of their relevant parameters has long been a focus of researchers (Hou et al., 2024). In physical icing models, the ice accretion rate on transmission lines is typically determined by the collision efficiency, collection efficiency, and freezing efficiency of supercooled raindrops. Among these, collection efficiency has long been regarded as a challenging and overlooked aspect of research. In recent years, although some progress has been made in calculating collection efficiency through numerical simulations and artificial intelligence applications, there are still significant deficiencies in experimental observations and theoretical modeling of the collection efficiency mechanism. Makkonen and Stallabrass (2019) have utilized high-speed photography to observe droplet impact dynamics, which improves the accuracy of droplet velocity measurements but fails to accurately determine the collision angle of droplets impacting the transmission line surface. Jiang et al. have employed Laser diffraction-based characterization to measure the particle size

https://doi.org/10.5194/egusphere-2026-800
Preprint. Discussion started: 18 March 2026

distribution of raindrops in freezing rain; however, it's unable to measure the three-dimensional (3D) motion vector of single droplets (Jiang et al., 2021). Kringlebotn Nygaard et al. have modified the Makkonen model for wet snow accretion by introducing an adhesion parameterization scheme based on liquid water content, but it still could not describe the complex impact process of supercooled water droplets (Kringlebotn Nygaard et al., 2013). Liu et al. have introduced physics-informed neural networks (PINNs) to solve the icing flow field. Although the accuracy is high within the interpolation range, the model's extrapolation ability under high turbulence conditions is poor due to the lack of physical constraints for extreme splashing scenarios (Liu et al., 2024). Snaiki et al. have developed a neural network based on meta-heuristic optimization, which improves data fitting but relies on macroscopic observational data from meteorological stations and lacks an explanation of the micro-physical mechanisms of icing (Jamali et al., 2024). The computational fluid dynamics-discrete element method (CFD-DEM) coupled model established by Gao et al. considers the two-way coupling of micron-sized droplets and conductor vibration but neglected the shear effect of oblique droplet impact (Gao et al., 2024). In summary, current research on the collection efficiency of transmission line icing faces problems of missing measurements for wind speed, temperature, particle size, and collision angle, failing to comprehensively account for the combined effects of dynamic and thermodynamic factors during the icing process. Limited by these issues, existing icing collection rate models often exhibit errors exceeding 30% under complex operating conditions, making it difficult to meet the needs of practical prediction.

Digital holography technology records and reconstructs the interference patterns of light waves, and when combined with image processing technology, it can acquire information about particle number, size, shape, and spatial distribution (Gao, 2024; Javidi et al., 2021; Khodadad, 2024). This technology is not limited by particle shape. With the rapid development of computers and high-resolution CCD or CMOS sensors, it has been widely used in fields such as medical imaging (Huang and Cao, 2024; Mihaylova, 2024), holographic projection (Blinder et al., 2022), cloud microphysics (Chambers et al., 2024; Fuchs et al., 2025), non-destructive testing (Osten and Pedrini, 2022), and particle field measurement (Kumar and Hong, 2025; Yang et al., 2024). Building on this, this study employs a coaxial digital holographic 3D measurement system to achieve synchronous and precise measurement of the particle size distribution, spatial motion trajectory, and collision angle of supercooled raindrops. Based on these measurements, this paper constructs a multi-stage coupled icing collection efficiency model, which integrates the dynamic collision process with the thermodynamic solidification process. This model overcomes the limitation of traditional isolated models, which are only applicable to single scenarios. By comprehensively incorporating influencing factors (such as wind speed, temperature, particle size, and collision angle) into the prediction, the error in predicting icing collection efficiency under complex working conditions is successfully reduced to within 3.5%. This provides powerful technical support for early warning and protection against transmission line icing.

https://doi.org/10.5194/egusphere-2026-800
Preprint. Discussion started: 18 March 2026

2 Theoretical background

Transmission line icing is fundamentally a dynamic process, in which supercooled raindrops collide with the conductor, then adhere, and finally freeze and accumulate. The outcome of a supercooled droplet's impact is jointly determined by both the dynamic attachment process and the thermal freezing process (Fu et al., 2006).

The dynamic attachment of a supercooled droplet to the conductor depends on the competition between inertia and surface tension (Zhang et al., 2020). When a droplet strikes the conductor at a given speed, inertia drives it to diffuse along the surface of the conductor into a thin film, while the surface tension of the droplet resists diffusion and tends to pull the droplet back into a spherical shape. The relative strength of these two effects can be characterized by the dimensionless Weber number (We), defined as the ratio of the droplet's kinetic energy upon impact to the surface tension's restorative energy. In other words, the Weber number represents the magnitude of inertial force relative to the capillary force. The Weber number can be expressed as:

$$We = \frac{\rho(v\sin\theta)^2 d}{\sigma}, \tag{1}$$

Where ρ is the droplet density, v is the incoming velocity of the droplet, d is the droplet diameter, θ is the angle between the droplet's velocity vector and the wire's surface normal, and σ is the surface tension. The Weber number quantifies the degree to which the droplet's kinetic energy drives diffusion deformation upon impact: when $We > 1$, inertia dominates and the droplet will completely diffuse and may even splash and break up; when $We \le 1$, the surface tension prevails and the droplet tends to remain intact and adhere. Under the competition between inertia and capillarity, a critical Weber number We_{cr} serves as the criterion for whether the droplet will adhere. If $We < We_{cr}$, the droplet can fully adhere to the surface; If $We > We_{cr}$, the droplet will fragment and splash, failing to adhere.

The core of the thermal freezing process lies in the heat transfer and equilibrium when a supercooled droplet undergoes liquid-solid phase change upon contacting the surface of the subfreezing conductor. Once a droplet attaches to a conductor surface below 0 °C, the supercooling ΔT drives heat transfer from the droplet to the conductor at the solid-liquid interface, eliminating the latent heat released by the droplet during freezing. For a droplet to freeze completely, the rate of heat conduction must balance the rate of the latent heat release, so as to remove all the latent heat prior to droplet detaches. The different dimensions of the heat conduction rate and the total latent heat, make it hard to compare them directly. Therefore, the effective contact time t_c (the time the droplet remains attached to the conductor) and the minimum freezing time t_f (the minimum time required for the droplet to solidify) are introduced. The freezing time of a droplet is directly proportional to the square of its characteristic size and inversely proportional to its degree of supercooling. Accordingly, a dimensional analysis gives the approximate relation:

$$t_f \approx \frac{\rho L d^2}{k\Delta T}, \tag{2}$$

https://doi.org/10.5194/egusphere-2026-800
Preprint. Discussion started: 18 March 2026

Where L is the latent heat of fusion of water (per unit volume) and k is the thermal conductivity. Equation (2) indicates that the freezing time can be prolonged by larger droplets while shortened by a greater ambient supercooling. Therefore, the success criterion for the thermal phase lies in that the droplet must be completely frozen before separate, namely, the effective contact time of the droplet must be greater than or equal to its minimum freezing time.

In summary, only by precisely obtaining key physical parameters of the supercooled droplets - such as their size, impact velocity, and collision angle - can the sticking efficiency be calculated accurately. For this purpose, a coaxial digital holographic 3D measurement system is used to measure these parameters.

Coaxial digital holography offers a simple optical setup, high information density, and minimal dual image interference in the far field, enabling its extensive application in recording and reconstructing three dimensional dynamic fields (Chen et al., 2021; Liu et al., 2021; Zhou, 2024). When a planar laser wave illuminates the particle field, the light diffracted by a particle (object beam) will interfere with the undisturbed reference beam. The interference pattern is recorded as a digital hologram. Afterwards, using the Fresnel-Kirchhoff diffraction formula, the object wave can be numerically reconstructed. According to scalar diffraction theory, if the measurement volume contains n particles, the reconstructed wave field $U_R(u,v)$ (Goodman, 1968; Gao et al., 2021) at the reconstruction plane coordinates (u,v) is given by the follows:

$$U_R(u,v)=\frac{1}{\mathrm{j}\lambda}\iint_{\infty} R(x,y)I_H(x,y)\frac{\exp\left(\mathrm{j}k\sqrt{(u-x)^2+(v-y)^2+z_r^2}\right)}{\sqrt{(u-x)^2+(v-y)^2+z_r^2}}\mathrm{d}x\mathrm{d}y \quad , \tag{3}$$

Where λ is the laser wavelength; $R(x,y)$ is the reference wave; $I_H(x,y)$ is the intensity of the interference fringes of the hologram; k is the wavenumber; x and y are the horizontal and vertical coordinates in the particle focal plane, respectively; u and v are the horizontal and vertical coordinates in the hologram reconstruction plane, respectively; and $z_r = z_{\mathrm{i}}(i=1,2,3\cdots)$ are reconstruction distances. A particle located at a reconstruction distance z_r will be focused on the reconstruction plane. By reconstructing the hologram at a series of different distances z_r, information about all particles within the sampled volume can be obtained. By applying an image fusion technique - specifically, a grayscale gradient variance method combined with a third-order Laplacian pyramid fusion algorithm - to the reconstructed digital images, the droplet particle sizes and three-dimensional positions can be measured with high accuracy. The application of a particle image recognition algorithm to the particles in the sampled volume yields the particle count.

By recording the time series of holograms through multiple exposures, the motion trajectories of the droplets can be obtained. In the reconstructed sequential particle images, each particle is tagged frame by frame and its 3D coordinates (x,y,z,t) are extracted. The displacement of a particle between two successive frames is:

$$\Delta s=\sqrt{(x_i-x_{i+1})^2\Delta x^2+(y_i-y_{i+1})^2\Delta y^2+(z_i-z_{i+1})^2\Delta z^2} \quad , \tag{4}$$

https://doi.org/10.5194/egusphere-2026-800
Preprint. Discussion started: 18 March 2026

from which the instantaneous droplet impact velocity can be determined using particle tracking velocimetry as:

$$v = \frac{\Delta s}{\Delta t}, \tag{5}$$

Where Δt is the exposure time interval between adjacent frames. Using the above method, the droplet's diameter, collision angle, and impact velocity can be accurately measured. These high-precision measurements provide reliable input parameters for the subsequent development of the sticking efficiency model.

3 Experimental setup

As shown in Fig. 1, a laboratory system is constructed to study the impact of micron-scale droplets on a conductor. The system is divided into two main parts: the first part is a coaxial digital holography measurement system consisting of a laser, a high-speed camera, and lenses. In the three experiments, a pulsed laser beam is expanded by lens L1 and then collimated into a parallel beam by lens L2, thereby illuminating the space containing simulated raindrops. The diffracted light produced by the particles interferes with the unblocked reference light, forming a coaxial digital hologram of the spray particle field. After propagating a certain distance, the hologram is imaged by a telecentric lens, recorded by the high-speed camera, and then stored on a computer. As shown in Fig. 2, after numerical reconstruction processing, the morphology and three-dimensional positions of the particles in the hologram can be recovered. The second part of the system is a simulated rainfall experimental setup, encompassing a droplet generator, a driving mechanism, and a support structure. Ultrapure water is pre-cooled to a supercooled state and placed in a pressurized chamber. A solenoid injection valve controls the pressure of a nitrogen tank, forcing supercooled water out of a nozzle to produce droplets with a certain velocity (1-8 m/s). By using nozzles of different diameters, supercooled droplets with diameters within the range 500-3000 μm can be generated. The laboratory temperature control system can maintain the ambient temperature between -20 °C and 0 °C (with ±1 °C accuracy). In the experiments, droplet impact and splashing tests were conducted on different combinations of impact velocity and angle, with droplet impact speed and collision angle as variables. Each set of conditions was repeated at least 5 times to ensure data reliability, and representative valid data were selected for analysis.

https://doi.org/10.5194/egusphere-2026-800
Preprint. Discussion started: 18 March 2026

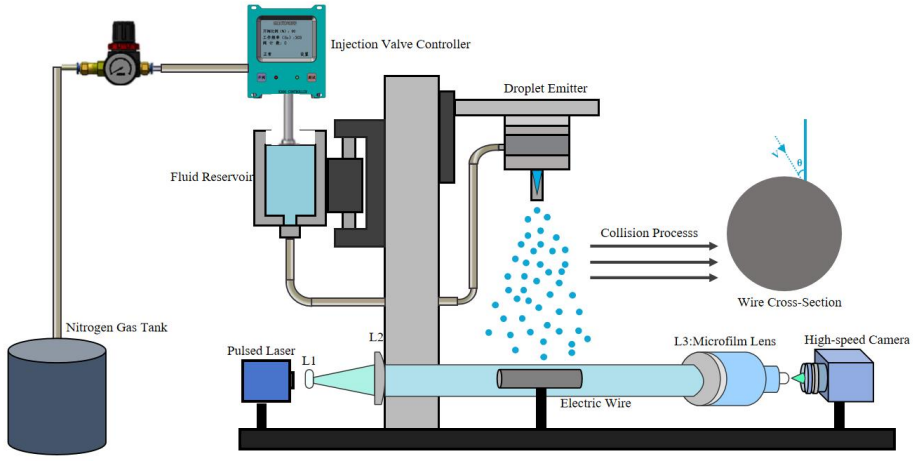

Figure 1: Experimental system for droplet impact on a power line.

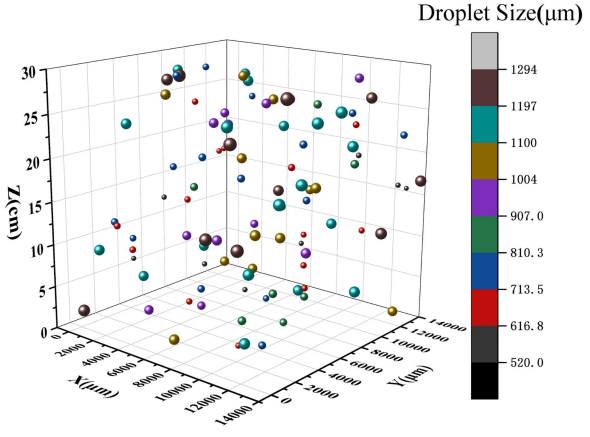

Figure 2: Three-dimensional spatial distribution of droplets.

The processing workflow for digital holograms and velocity extraction is shown in Fig. 3, including hologram numerical reconstruction, depth-of-field extension, image fusion, particle identification, particle labeling, and velocity calculation steps. Using the above techniques, the splashing process of a group of micron-scale droplets impacting the conductor was measured and reconstructed, as illustrated in Fig. 4. Image recognition determines that the droplet diameter in this case reaches approximately 1100 μm. The analysis of the reconstructed trajectory has yielded a collision angle of about 70°, with an impact velocity of 2.5 m/s.

https://doi.org/10.5194/egusphere-2026-800
Preprint. Discussion started: 18 March 2026

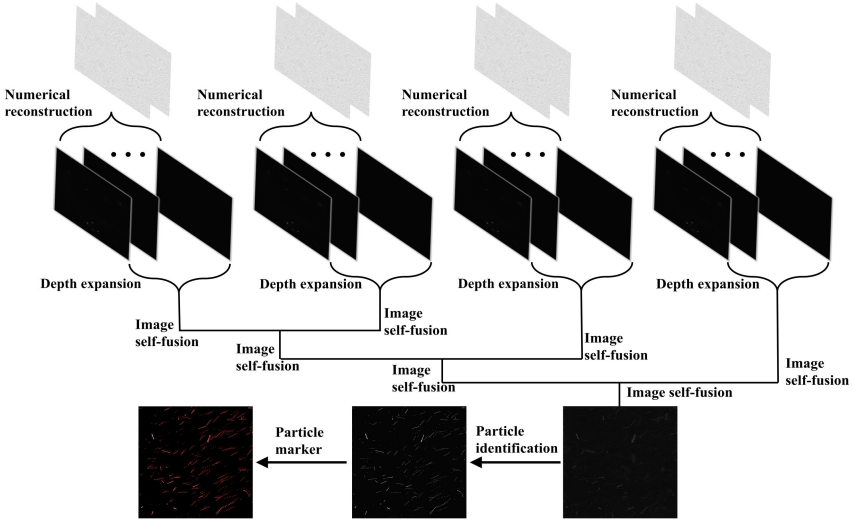

Figure 3: Hologram processing flow.

https://doi.org/10.5194/egusphere-2026-800
Preprint. Discussion started: 18 March 2026

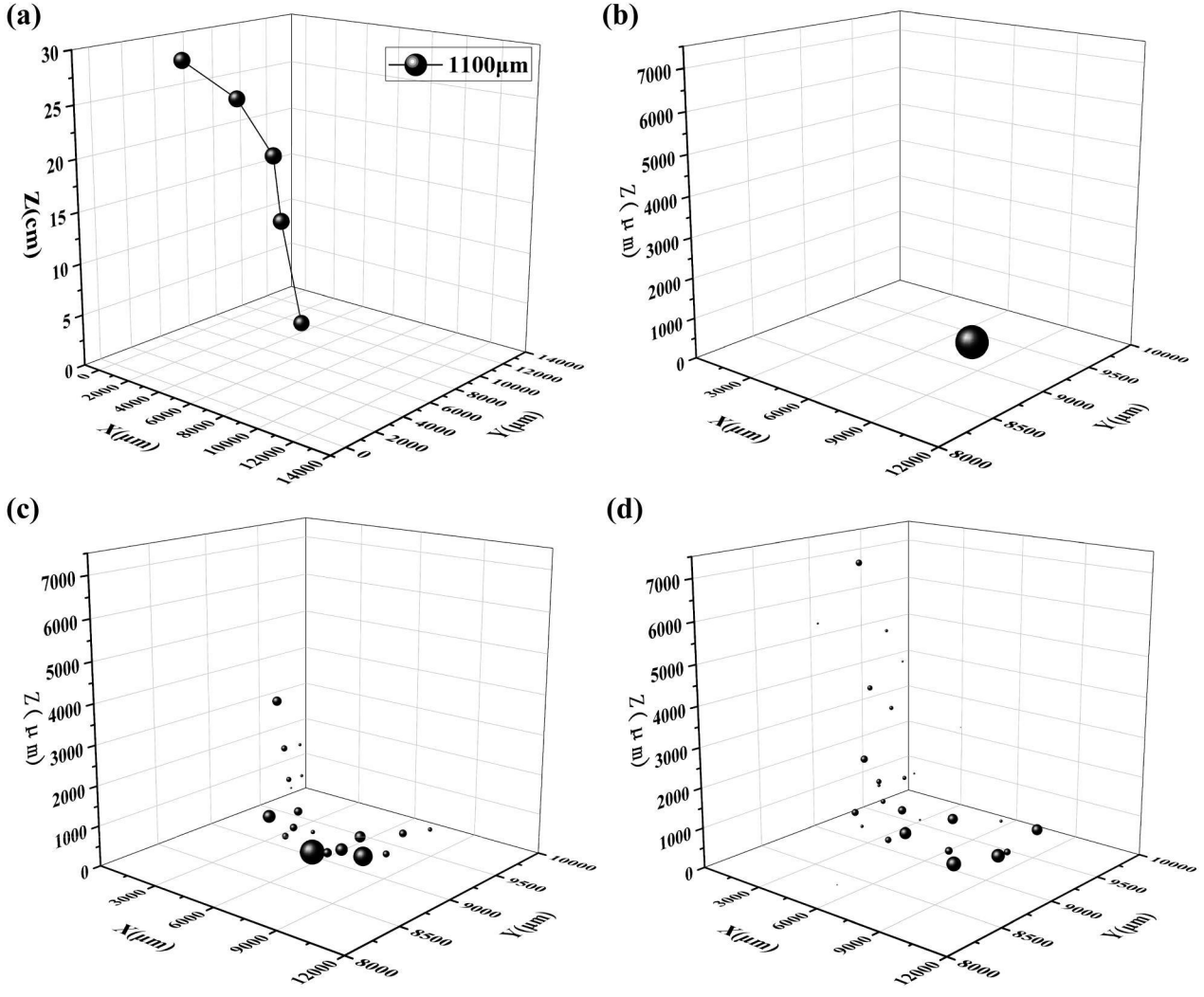

Figure 4: Droplet trajectory and splashing process upon impacting the transmission line. (a)Droplet falling trajectory (b)Time-sequential diagram of particle breakage process:t=0. (c)Time-sequential diagram of particle breakage process:t=0.5ms (d)Time-sequential diagram of particle breakage process:t=1ms.

4 Development and validation of the sticking efficiency model

4.1 Model development

4.1.1 Dynamic phase

For cases with an incoming wind, droplets strike the conductor at some relative collision angle θ instead of a perpendicular approach. When a droplet impacts the surface of a cylindrical conductor at a velocity v_d and collision angle θ, the tangential

https://doi.org/10.5194/egusphere-2026-800
Preprint. Discussion started: 18 March 2026

component of its velocity will induce the droplet to slide and be stripped along the conductor surface, whereas the normal component of velocity is the key driving force targeting the deformation and breakup of droplets. Therefore, during the development progress of the dynamic model, the influence of the normal velocity component on the droplet's attachment behavior should be focused on. The normal impact velocity is defined as:

$$v_n = v_d \cdot \sin\theta \,, \tag{6}$$

The traditional Weber number formulation is only applicable to the perpendicular impact of droplets, and therefore cannot quantify the shear effect in oblique impact of supercooled droplets under high wind speeds. Experiments show that when the collision angle θ is reduced from 90° to 60°, as illustrated in Fig. 5, the observed droplet splashing probability increases by about 10-25%, indicating that smaller collision angle will lead to more pronounced airflow shear effect, and increased possibility of the droplet to splash rather than adhere.

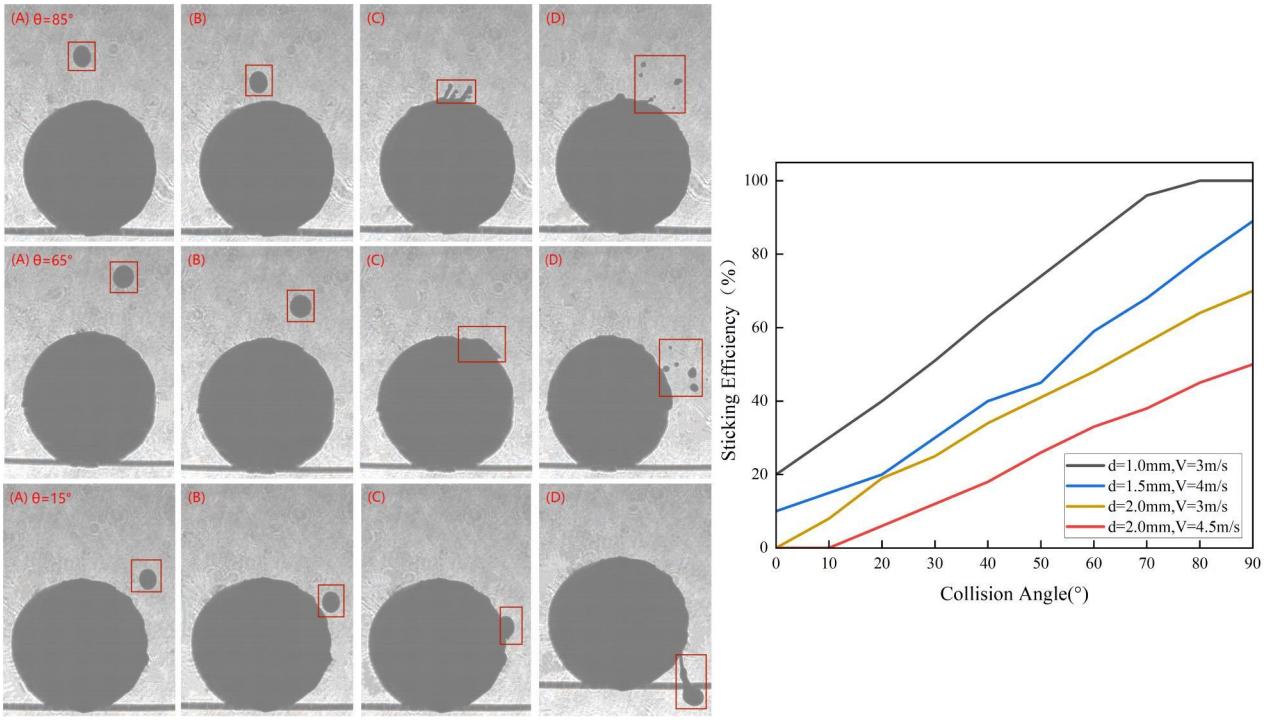

Figure 5: Variation of droplet sticking efficiency for impacts at different collision angles.

To quantitatively describe the effect of collision angle on the droplet's dynamic behavior, an effective Weber number We_{eff} is introduced to modify the original Weber number. The shear-enhanced effective Weber number model is proposed as follows:

https://doi.org/10.5194/egusphere-2026-800
Preprint. Discussion started: 18 March 2026

$$We_{\text{eff}} = \frac{\rho_d v_n^2 d}{\sigma} \cdot \left[1 + \lambda \left(\frac{90^\circ - \theta}{90^\circ} \right)^2 \right], \tag{7}$$

Where ρ is the droplet density, v_n is the normal impact velocity, d is the droplet diameter, and σ is the surface tension of water. λ is an oblique-impact correction factor. Experimental analysis shows that when a droplet collides at a certain angle, the asymmetric impact forces reduce the effective surface tension threshold by roughly 10%, hence $\lambda \approx 0.1$.

As shown in Fig. 6 and Fig. 7, the analysis of high-speed camera data reveals that higher impact velocities will produce a stronger kinetic impulse, promoting droplet splashing; Under the same wind speed and collision angle conditions, smaller droplets will embrace a noticeably higher adhesion rate than larger droplets. These experimental trends indicate that the critical Weber number We_{cr} is influenced by the nonlinear coupling of collision angle θ, droplet diameter d, and droplet impact velocity v_{d}.

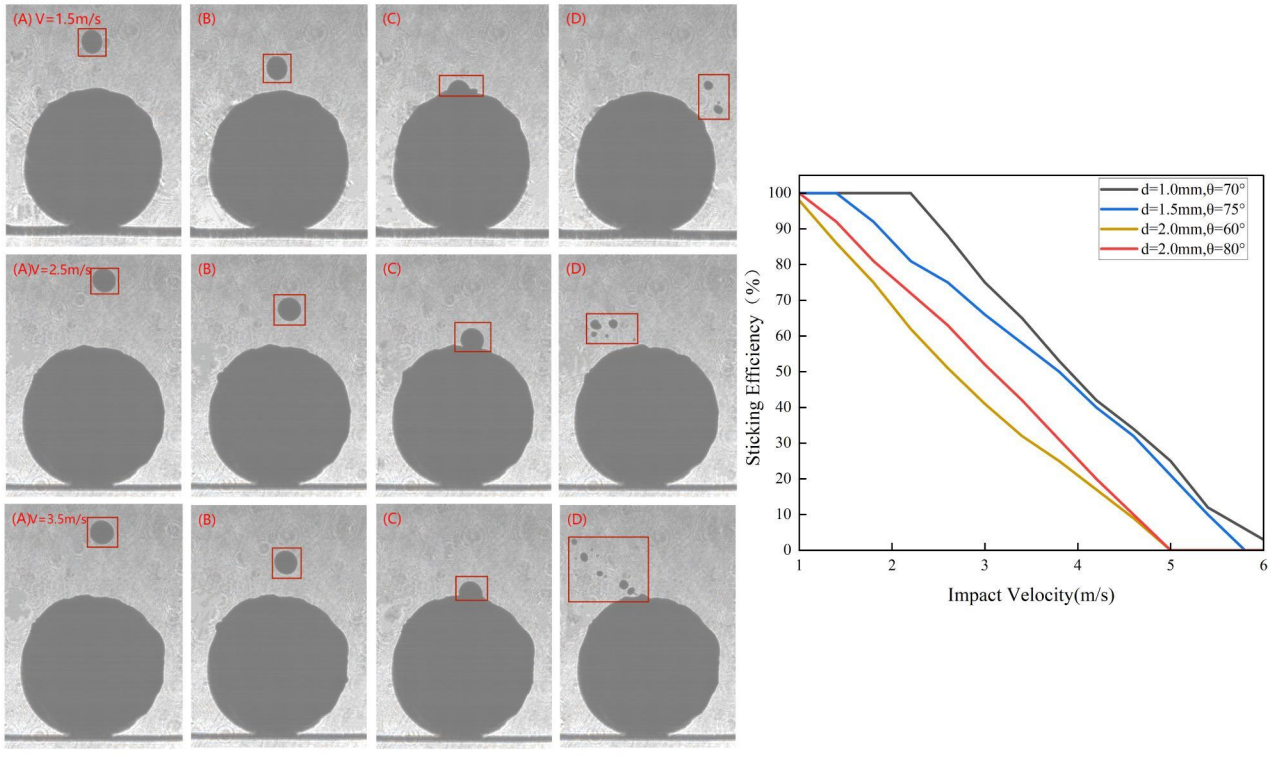

Figure 6: Variation of droplet sticking efficiency with different impact velocities.

https://doi.org/10.5194/egusphere-2026-800
Preprint. Discussion started: 18 March 2026

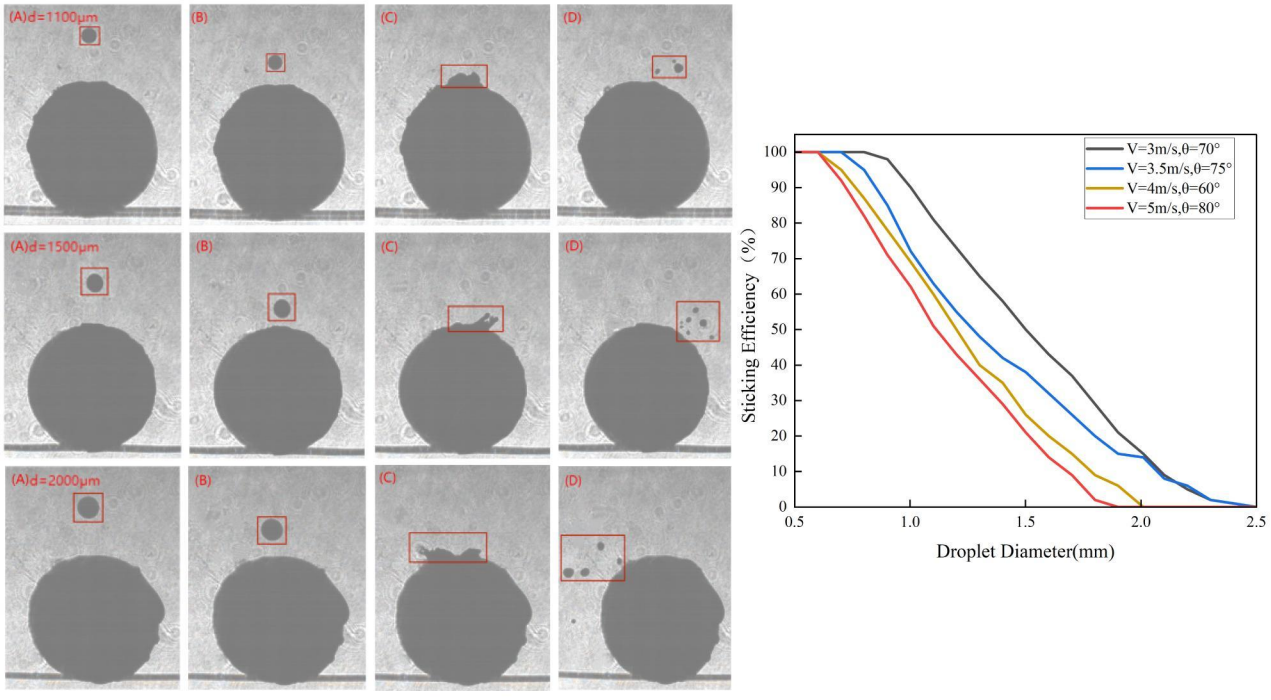

195 **Figure 7:** Variation of droplet sticking efficiency with different droplet diameters.

Accordingly, by performing a ternary nonlinear fitting on the experimental data, the modified critical Weber number model is introduced as follows:

$$We_{cr} = C(1 - Ad)(1 - Bv_{\mathrm{n}}{}^{\delta})(1 - \cos\theta)\,, \tag{8}$$

Where C is a baseline constant, A and B are empirical fitting coefficients, and δ is the velocity influence exponent.
200 Experimental calibration: $C = 745$, $A = 0.02$, $B = 0.012$, and $\delta = 1.8$.

Based on the criterion of inertia vs. surface tension competition, the ratio of the effective Weber number to the critical Weber number determines the outcome of droplet attachment. The dynamic attachment probability P_s is defined as a piecewise function of this ratio:

$$P_s(\theta, d, v) = \begin{cases} 1, & We_{eff} < 0.3We_{cr} \\ \dfrac{We_{cr} - We_{eff}}{0.7We_{cr}}, & 0.3We_{cr} \le We_{eff} \le We_{cr} \\ 0, & We_{eff} > We_{cr} \end{cases}, \tag{9}$$

https://doi.org/10.5194/egusphere-2026-800
Preprint. Discussion started: 18 March 2026

4.1.2 Thermal phase

High-speed imaging measurements show that the effective contact time t_c increases with the increase of droplet diameter, and decreases with the increase of impact velocity. Therefore, the calculation of the effective contact time can be simplified as approximately:

$$t_c = \frac{d_d}{v_n}, \tag{10}$$

Traditional models of liquid-solid phase change time typically assume ideal heat conduction, considering only the supercooling ΔT as a variable. In reality, however, there is a micrometer-scale oxide layer and an air boundary layer on the conductor surface, significantly inhibiting heat flow. In this study, the kinetic energy of the impacting droplet can disrupt the air film on the conductor surface and increase the actual contact area between the droplet and the conductor; Such effect grows quadratically with v_n. Therefore, the expression for the liquid-to-solid phase change time is reconstructed to account for kinetic-energy-enhanced heat transfer:

$$t_f = \frac{\rho L d^2}{h_i \Delta T A_c (1+\beta v_n^2)}, \tag{11}$$

Where ρ is the liquid density, L is the latent heat of fusion (volumetric latent heat release) of the liquid, and h_i is the average convective heat transfer coefficient between the droplet and the conductor (reflecting the heat transfer capability at the solid-liquid interface). $A_c = 1 + 0.8\sin\theta$ is a contact area correction factor introduced to approximate the effect of collision angle on the droplet's spreading contact area. β is the kinetic-energy enhancement coefficient for heat transfer, characterizing the effect of impact velocity on the freezing process; Our experimental analysis yielded $\beta \approx 0.05 \mathrm{s}^2/\mathrm{m}^2$.

Based on the relationship between t_c and t_f, the freezing probability P_f can be expressed as follows:

If $t_c \geq t_f$, there is sufficient time for heat transfer and the supercooled droplet will freeze completely ($P_f = 1$).

If $t_c < t_f$, the unfrozen portion of the droplet will be stripped away by the airflow. In this case, the freezing probability is given by:

$$P_f = \exp\left(-\frac{t_f}{t_c}\right), \tag{12}$$

4.1.3 Overall sticking efficiency calculation

The overall sticking efficiency η is essentially the coupled probability between the dynamic collision stage and the thermal freezing stage that occur sequentially. Assuming that the dynamic attachment process and the thermal freezing process are independent, the total sticking efficiency can be expressed as the product of the probabilities of the two stages:

https://doi.org/10.5194/egusphere-2026-800
Preprint. Discussion started: 18 March 2026

$$\eta = P_s \cdot P_f , \tag{13}$$

4.2 Model validation

To rigorously evaluate the accuracy and applicability of the proposed model, three representative sticking efficiency models were selected for comparative analysis: the Jones model (Jones, 1996), the Makkonen model (Makkonen, 2000), and the Mundo-Sommerfeld-Tropea splashing model (Mundo et al., 1995). Using both controlled laboratory experiments and inverse analysis of actual transmission line icing accident data, the prediction accuracy of the sticking efficiency model proposed in this work was evaluated.

4.2.1 Experimental design

(1) Laboratory parameters: The laboratory experiments were designed with five factors (droplet diameter, impact velocity, collision angle, supercooling, and crosswind speed), each at three levels, as summarized in Table 1. This yields $3^5 = 243$ unique test conditions; Each condition was repeated 3 times, for a total of 729 experiments.

Table 1: Experimental parameters

Variable	Values	Uni
Droplet diameter d	800,1200,2000	μm
Impact velocity v	2,5,8	m/s
Collision angle θ	30, 60, 85	° (degrees)
Supercooling ΔT	5,10,15	°C
Crosswind speed v_w	0,4,8	m/s

(2) Actual transmission line icing cases: The model using three real-world icing incident cases on transmission lines was also evaluated. In each case, the measured sticking efficiency η_{true} (based on field observations) is given, along with the prevailing environmental parameters.

Case 1: Parameters: collision angle $\theta = 55^\circ$, droplet diameter $d = 1120\mu m$, droplet velocity $v = 6.5\ \text{m/s}$, supercooling $\Delta T = 7^\circ\text{C}$, crosswind speed $v_w = 3\ \text{m/s}$.

Case 2: Parameters: $\theta = 38^\circ$, $d = 1850\mu m$, $v = 11.2\ \text{m/s}$, $\Delta T = 6.5^\circ\text{C}$, $v_w = 14\ \text{m/s}$.

Case 3: Parameters: $\theta = 75^\circ$, $d = 800\mu m$, $v = 4\ \text{m/s}$, $\Delta T = 12^\circ\text{C}$, $v_w = 1\ \text{m/s}$.

4.2.2 Results analysis

Using the above experimental data, the comparison was conducted on the sticking efficiency results calculated by each model (see Fig. 8), and the prediction errors of each model under the actual icing scenarios (see Figs. 9-11). The results show that the sticking

https://doi.org/10.5194/egusphere-2026-800
Preprint. Discussion started: 18 March 2026

efficiency model proposed in this paper outperforms in terms of accuracy, applicability, and stability. The model can make an effective prediction on the icing sticking efficiency under different combinations of temperature, wind speed, droplet size, and collision angle. Even in complex and harsh environments such as heavy precipitation with high winds and low temperatures, the prediction error of our model remains within 3.5%, superior to the predictive performance of existing classical models.

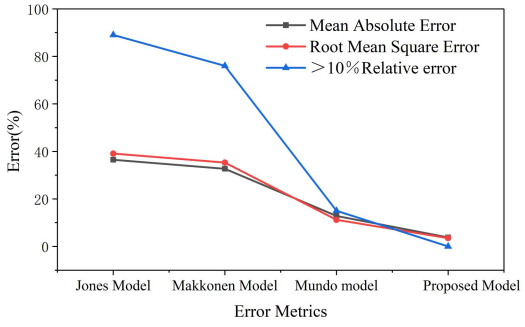

Figure 8: Sticking efficiency results calculated by various models using the laboratory data.

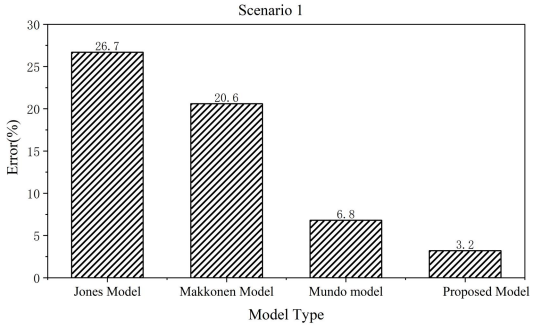

Figure 9: Comparison of sticking efficiency prediction errors for actual case 1.

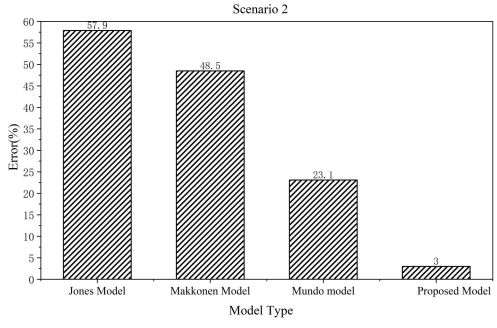

https://doi.org/10.5194/egusphere-2026-800
Preprint. Discussion started: 18 March 2026

Figure 10: Comparison of sticking efficiency prediction errors for actual case 2.

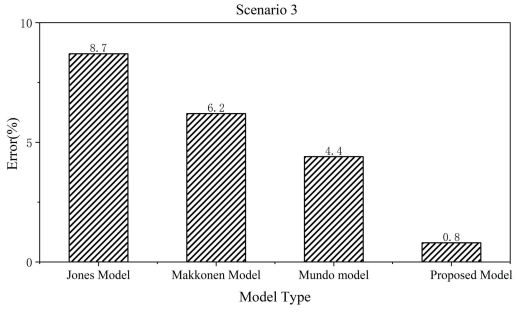

Figure 11: Comparison of sticking efficiency prediction errors for actual case 3.

5 Conclusions

In this study, a coaxial digital holographic three-dimensional measurement system was employed to achieve synchronized and high-precision measurements of supercooled droplet size distributions, spatial motion trajectories, and impact angles. Such measurement has lifted the limitations of traditional two dimensional projection measurements, addressed the problems of missing motion vector information and missing detections of tiny droplets, and provided accurate physical parameter inputs for the sticking efficiency model. On this basis, a droplet icing sticking efficiency prediction model was developed, which couples the dynamic collision process and the thermal freezing process in multiple stages. Through the comprehensive consideration on factors including wind speed, temperature, droplet size, and collision angle, the model was capable of eliminating the limitation of only handling a single scenario in traditional models. Under complex environmental conditions (such as high wind, intense precipitation, and low temperature), our model has successfully controlled the sticking efficiency prediction error within 3.5%, with a superior prediction accuracy to existing models. Laboratory simulation tests and validations against typical icing accident cases demonstrate that even under extreme conditions (e.g. mixed wind and rain, high turbulence), the model maintains excellent predictive accuracy and stability. This study lays a theoretical and technical foundation for online monitoring and early warning of transmission line icing, which is of great significance for ensuring the safe operation of the power grid.

Code availability

Not applicable.

Data availability

The data that support the findings of this study are available from the corresponding author upon reasonable request.

https://doi.org/10.5194/egusphere-2026-800
Preprint. Discussion started: 18 March 2026

Team list

Not applicable.

Author contributions

PZh and DH designed the experiments, and JC carried them out. PZ and JW developed the model code and performed the simulations. JL and XX calibrated and preprocessed the raw data. YM performed data curation. Pu Zhang prepared the manuscript with contributions from all co-authors.

Competing interests

The authors declare that they have no conflict of interest.

Disclaimer

Copernicus Publications remains neutral with regard to jurisdictional claims made in the text, published maps, institutional affiliations, or any other geographical representation in this paper. While Copernicus Publications makes every effort to include appropriate place names, the final responsibility lies with the authors. Views expressed in the text are those of the authors and do not necessarily reflect the views of the publisher.

Acknowledgements

The authors would like to thank Xi'an University of Technology for the support and assistance provided during the research. The research infrastructure relied on in this study is the Beijing Comprehensive Test Base Laboratory of Weather Modification, and the authors express their gratitude for the platform and technical support offered by the laboratory.

Financial support

This work was supported by the National Natural Science Foundation of China (Nos. 42375126 and 42375137).

References

Blinder, D., Birnbaum, T., Ito, T., and Shimobaba, T.: The state-of-the-art in computer generated holography for 3D display, Light Adv. Manuf., 3, 35, https://doi.org/10.37188/lam.2022.035, 2022.

Chambers, T. E., Reid, I. M., and Hamilton, M.: A lightweight holographic imager for cloud microphysical studies from an untethered balloon, Atmos. Meas. Tech., 17, 3237-3253, https://doi.org/10.5194/amt-17-3237-2024, 2024.

Chen, N., Wang, C., and Heidrich, W.: Snapshot space-time holographic 3D particle tracking velocimetry, Laser Photonics Rev., 15, 2100008, https://doi.org/10.1002/lpor.202100008, 2021.

https://doi.org/10.5194/egusphere-2026-800
Preprint. Discussion started: 18 March 2026

Fuchs, C., Ramelli, F., Schweizer, D., Lohmann, U., and Henneberger, J.: Putting the spotlight on small cloud droplets with SmHOLIMO -a new holographic imager for in situ measurements of clouds, Atmos. Meas. Tech., 18, 2969-2986, https://doi.org/10.5194/amt-18-2969-2025, 2025.

Fu, P., Farzaneh, M., and Bouchard, G.: Two-dimensional modelling of the ice accretion process on transmission line wires and conductors, Cold Reg. Sci. Technol., 46, 132-146, https://doi.org/10.1016/j.coldregions.2006.06.004, 2006.

Gao, P.: Observation method of three-dimensional particle velocity based on digital holography, MD thesis, Xi'an University of Technology, Xi'an, China, 2024.

Gao, P., Wang, J., Zhao, C. C., Tang, J. B., Liu, J. J., Yan, Q., and Hua, D. X.: Simultaneous measurement method of cloud microphysical parameters based on digital holographic interferometry, Acta Phys. Sin., 70, 099201, https://doi.org/10.7498/aps.70.20201779, 2021.

Gao, W., Sato, Y., and Zhou, K.: CFD-DEM modeling of bidirectional coupling between micron droplets and conductor vibration, Powder Technol., 425, 118572, https://doi.org/10.1016/j.powtec.2023.118572, 2024.

Goodman, J. W.: Introduction to Fourier optics, McGraw-Hill, New York, USA, 1968.

Hou, H., Wang, Y., Bai, X., Lv, J., Cui, R., Zhang, L., and Li, S.: Modelling icing growth on overhead transmission lines: Current advances and future directions, Energy Convers. Econ., 5, 062001, https://doi.org/10.1049/enc2.12131, 2024.

Huang, Z. and Cao, L.: Quantitative phase imaging based on holography: trends and new perspectives, Light Sci. Appl., 13, 145, https://doi.org/10.1038/s41377-024-01453-x, 2024.

Snaiki, R., Jamali, A., Rahem, A., Shabani, M., and Barjenbruch, B. L.: A metaheuristic-optimization-based neural network for icing prediction on transmission lines, Cold Reg. Sci. Technol., 224, 104249, https://doi.org/10.1016/j.coldregions.2024.104249, 2024.

Javidi, B., Carnicer, A., Anand, A., Barbastathis, G., Chen, W., Ferraro, P., Goodman, J., Horisaki, R., Khare, K., Kujawinska, M., and Leitgeb, R. A.: Roadmap on digital holography, Opt. Express, 29, 35078-35118, https://doi.org/10.1364/OE.435915, 2021.

Jiang, X., Wang, Z., and Liu, Y.: Laser diffraction-based characterization of raindrop size distribution in freezing precipitation, Atmos. Res., 259, 105682, https://doi.org/10.1016/j.atmosres.2021.105682, 2021.

Jones, K. F.: A simple model for freezing rain ice loads, Atmos. Res., 46, 87-97, https://doi.org/10.1016/S0169-8095(97)00053-7, 1996.

Khodadad, D.: Digital holography and its application, Appl. Sci., 14, 11254, https://doi.org/10.3390/app142311254, 2024.

Kringlebotn Nygaard, B. E., Ágústsson, H., and Somfalvi-Tóth, K.: Modeling wet snow accretion on power lines: Improvements to previous methods using 50 years of observations, J. Appl. Meteorol. Climatol., 52, 2189-2203, https://doi.org/10.1175/JAMC-D-12-0332.1, 2013.

Kumar, M. S. and Hong, J.: A review of 3D particle tracking and flow diagnostics using digital holography, Meas. Sci. Technol., 36, 032005, https://doi.org/10.1088/1361-6501/adabff, 2025.

https://doi.org/10.5194/egusphere-2026-800
Preprint. Discussion started: 18 March 2026

Liu, F., Chen, T., and Wu, J.: Physics-informed neural networks for predicting ice accretion on power lines, Appl. Energy, 350, 121890, https://doi.org/10.1016/j.apenergy.2023.121890, 2024.

Liu, Z., Takahashi, T., Lindsay, D., Thevar, T., Sangekar, M., Watanabe, H. K., Burns, N., Watson, J., and Thornton, B.: Digital in-line holography for large-volume analysis of vertical motion of microscale marine plankton and other particles, IEEE J. Oceanic Eng., 47, 789-801, https://doi.org/10.1109/JOE.2021.3066788, 2021.

Makkonen, L.: A model for the growth of rime, glaze and wet snow on structures, Phil. Trans. R. Soc. A, 358, 2913-2939, https://doi.org/10.1098/rsta.2000.0690, 2000.

Makkonen, L. and Stallabrass, J. R.: Two-dimensional high-speed imaging of droplet impact dynamics, J. Atmos. Oceanic Technol., 36, 1523-1534, https://doi.org/10.1175/JTECH-D-18-0184.1, 2019.

Mihaylova,E.M.:Imaging of live cells by digital holographic microscopy, Photonics, 11, 980, https://doi.org/10.3390/photonics11100980, 2024.

Mundo, C., Sommerfeld, M., and Tropea, C.: Droplet-wall collisions: experimental studies of the deformation and breakup processes, Int. J. Multiphase Flow, 21, 151-173, https://doi.org/10.1016/0301-9322(94)00069-V, 1995.

Osten, W. and Pedrini, G.: 55 Years of holographic non-destructive testing and experimental stress analysis: Is there still progress to be expected?, Light Adv. Manuf., 3, 121-136, https://doi.org/10.37188/lam.2022.008, 2022.

Wang, G., Shen, J., Jin, M., Huang, S., Li, Z., and Guo, X.: Prediction model for transmission line icing based on data assimilation and model integration, Front. Environ. Sci., 12, 1403426, https://doi.org/10.3389/fenvs.2024.1403426, 2024.

Yang, C. Y., Wang, J., Zhang, C., Zhou, H., Yang, J. S., Yue, Z. G., Liang, G., Liu, J. J., and Hua, D. X.: Observation method of cloud ice crystal microphysical parameters based on digital holography, Acta Optica Sin., 44, 0601017, https://doi.org/10.3788/AOS231067, 2024.

Zhang, X., Liu, X., Wu, X., and Min, J.: Impacting-freezing dynamics of a supercooled water droplet on a cold surface: Rebound and adhesion, Int. J. Heat Mass Transfer, 158, 119997, https://doi.org/10.1016/j.ijheatmasstransfer.2020.119997, 2020.

Zhou, H.: Hail recognition method and experimental research based on digital holography, MD thesis, Xi'an University of Technology, Xi'an, China, 2024.